Science Advances
AAAS

Supplementary Materials for

Locally controllable magnetic soft actuators with reprogrammable contraction-derived motions

Yahe Wu *et al.*

Corresponding author: Yan Ji, jiyan@mail.tsinghua.edu.cn; weiyen@tsinghua.edu.cn

Sci. Adv. **8**, eabo6021 (2022)
DOI: 10.1126/sciadv.abo6021

The PDF file includes:

Other Supplementary Material for this manuscript includes the following:

Supplementary Text

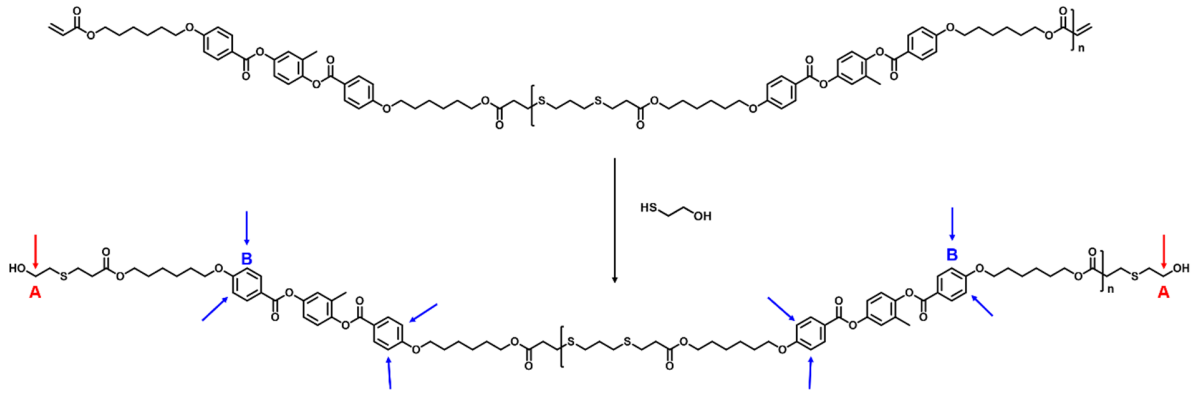

Fig. S1.

Chemical structure of hydroxyl-terminated LC oligomer.

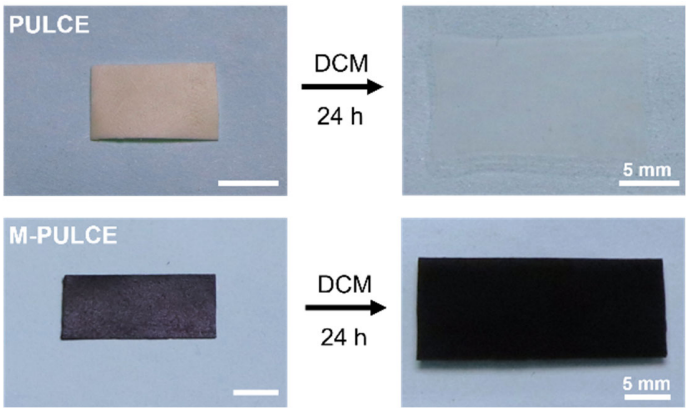

Fig. S2.

Images of the blank PULCE and M-PULCE-2 before and after swelling for 24 h.

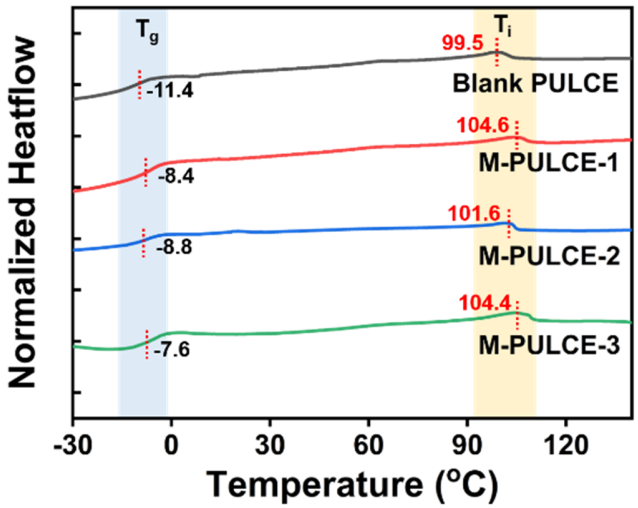

Fig. S3.

DSC curves of the blank PULCE and M-PULCEs.

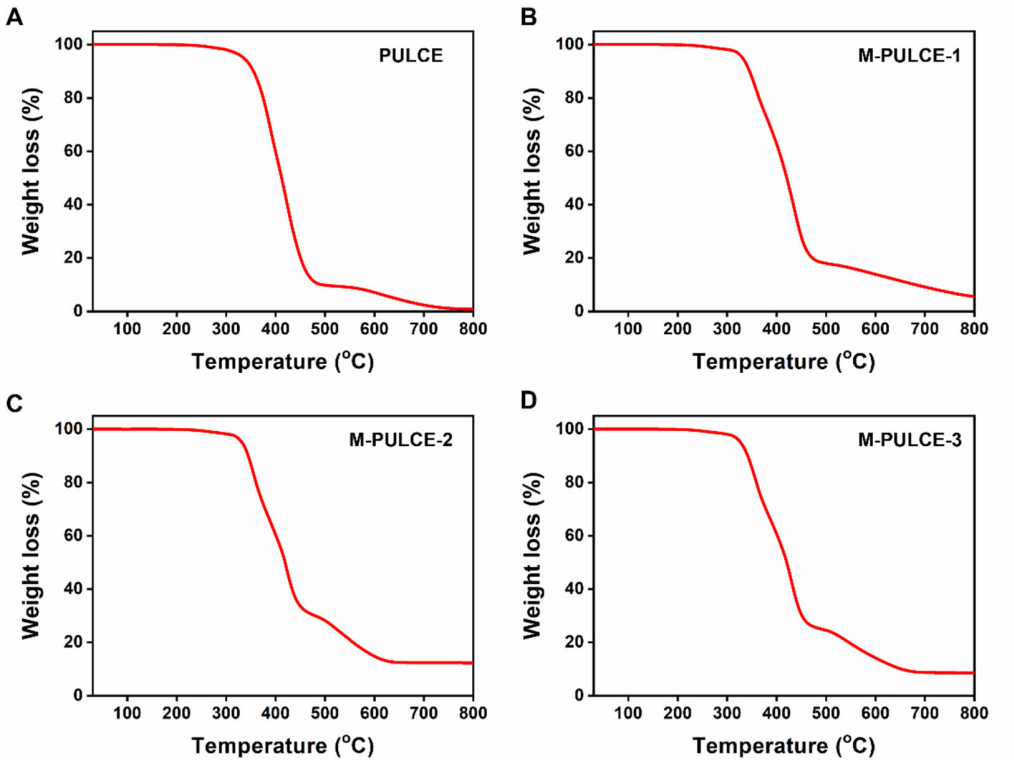

Fig. S4.

TGA curves of PULCE and M-PULCEs under N_2 atmosphere. (**A**) Blank PULCE. Temperature at 1% and 5% weight loss: 269 ºC and 335 ºC, respectively; (**B**) M-PULCE-1. Temperature at 1% and 5% weight loss: 265 ºC and 332 ºC, respectively; (**C**) M-PULCE-2. Temperature at 1% and 5% weight loss: 268 ºC and 332 ºC, respectively; (**D**) M-PULCE-3. Temperature at 1% and 5% weight loss: 261 ºC and 332 ºC, respectively.

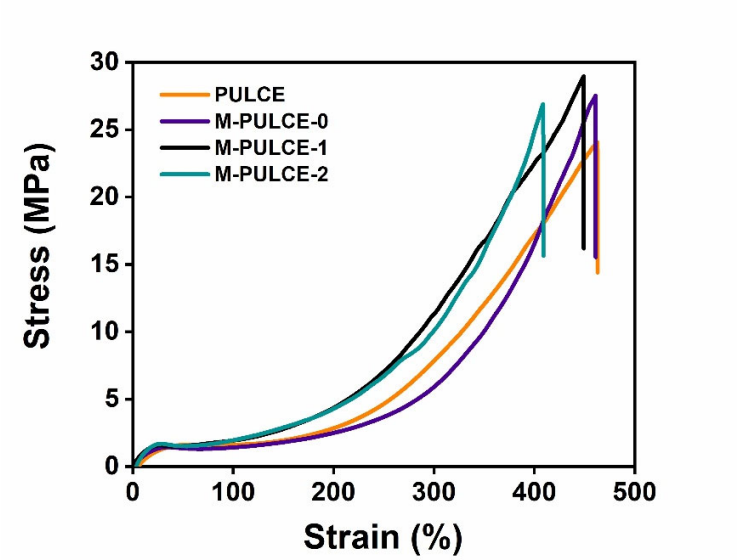

Fig. S5.

Stress-strain curves of PULCE and M-PULCEs.

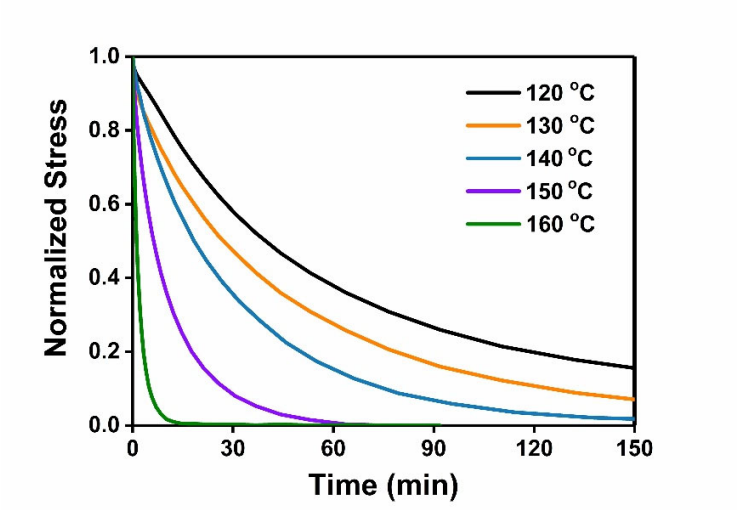

Fig. S6.

Normalized stress relaxation curves of PULCEs at different temperatures.

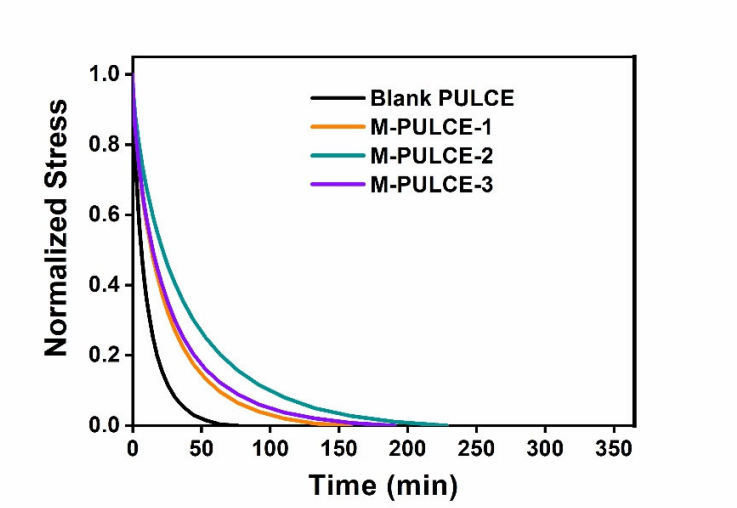

Fig. S7.

Normalized stress relaxation curves of M-PULCEs with different contents of Fe_3O_4 NPs at 150 ºC.

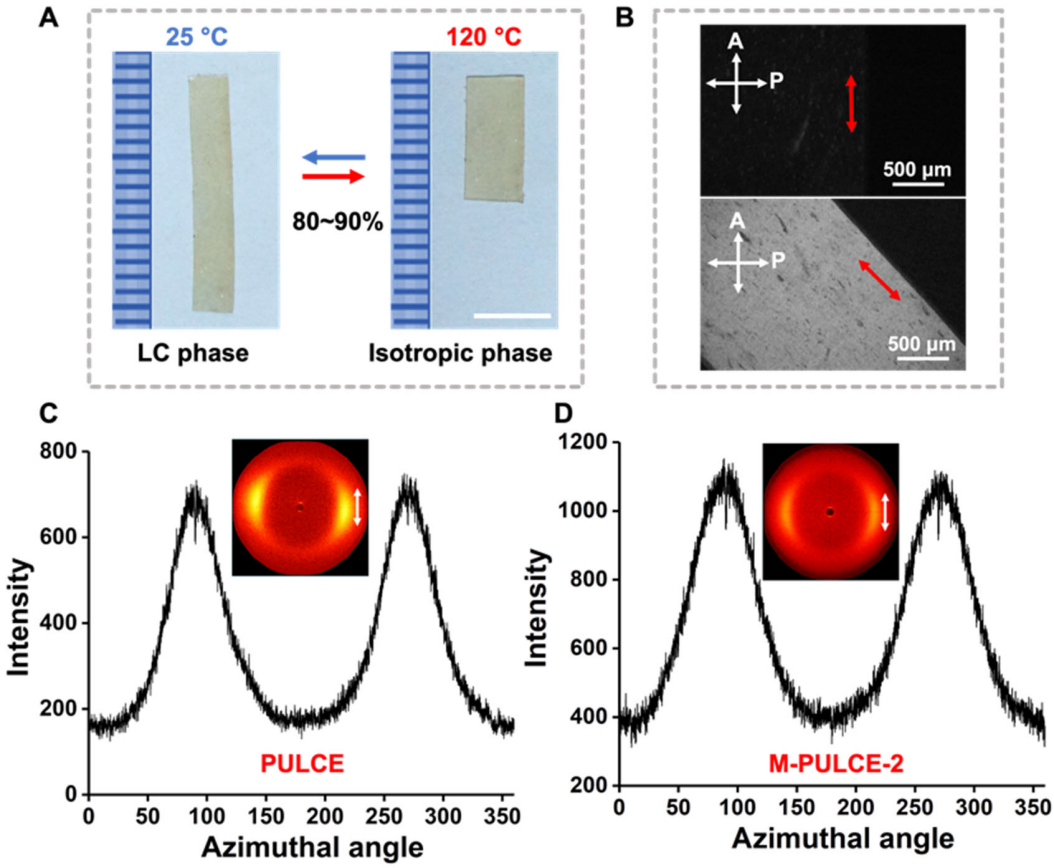

Fig. S8.

POM and XRD analysis of the monodomain PULCEs and M-PULCEs. (**A**) Reversible thermal actuation of PULCEs. (**B**) POM images of uniaxially aligned PULCE under crossed polarizers. The arrow denotes the aligning direction. (**C**) Azimuthal intensity scan of the uniaxially aligned PULCE film (actuation strain: 90%). Inset: 2D XRD patterns of the monodomain PULCE sample. The arrow denotes the aligning direction. The image showed a pair of arcs along the aligning direction, indicating a nematic phase. (**D**) Azimuthal intensity scan of the uniaxially aligned M-PULCE-2 film (actuation strain: 78%). Inset: 2D XRD patterns of the monodomain M-PULCE-2 sample. The arcs shown in the image indicate the nematic phase of M-PULCEs. The arrow denotes the aligning direction.

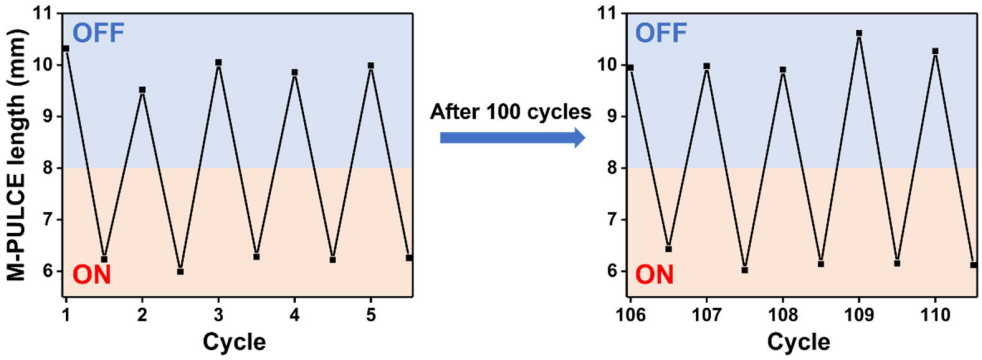

Fig. S9.

Actuation stability test of monodomain M-PULCE-2 for 110 magnetic actuation cycles under AMF. The temperature of the sample when AMF is on is around 120 ºC (f = 495 kHz; H = 158.27 Gs); when off, the temperature is in the range of 30~43 ºC. The length of the contractile actuator was measured at the first five cycles and the last five cycles.

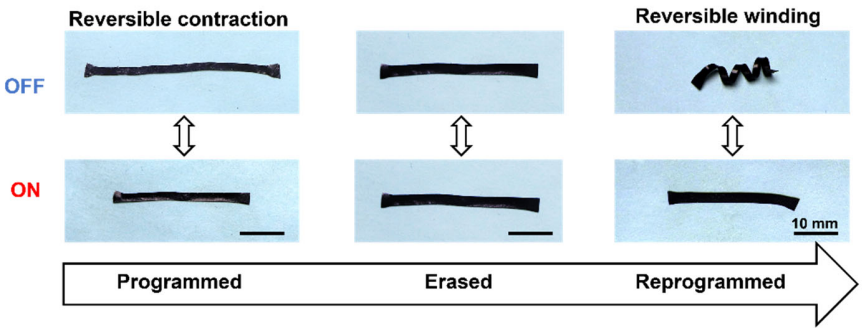

Fig. S10.

Reprogramming and erasure by heat. M-PULCE-2 was first programmed with reversible contraction motion, and then it was placed on the hot plate at 150 ºC for 60 minutes (erasure process). The erased sample showed no significant actuations under both heat and AMF. It was then reprogrammed with a reversible winding/unwinding motion.

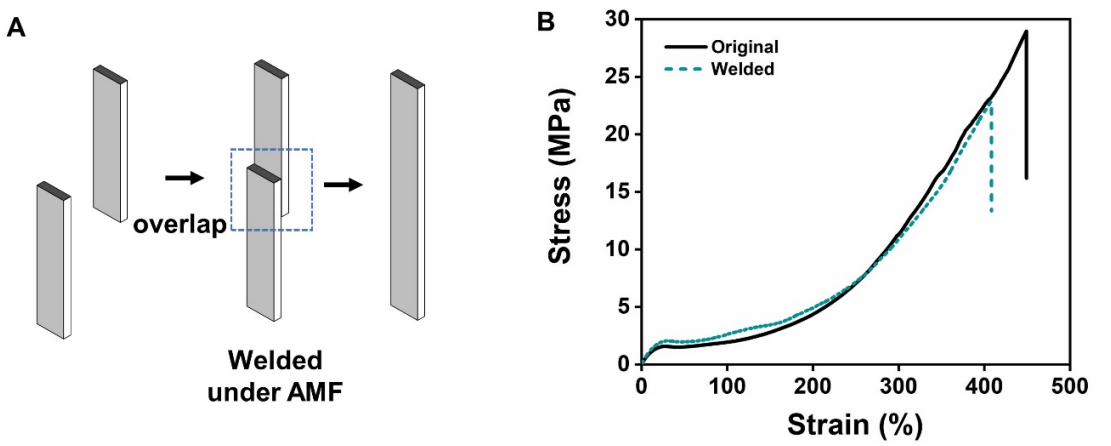

Fig. S11.

AMF-assisted welding of M-PULCEs. (**A**) Schematic illustration of AMF-assisted welding process. (**B**) Lap-shear test of the AMF-welded sample (M-PULCE-2; sample size: 2.25 mm × 0.40 mm (width × thickness)).

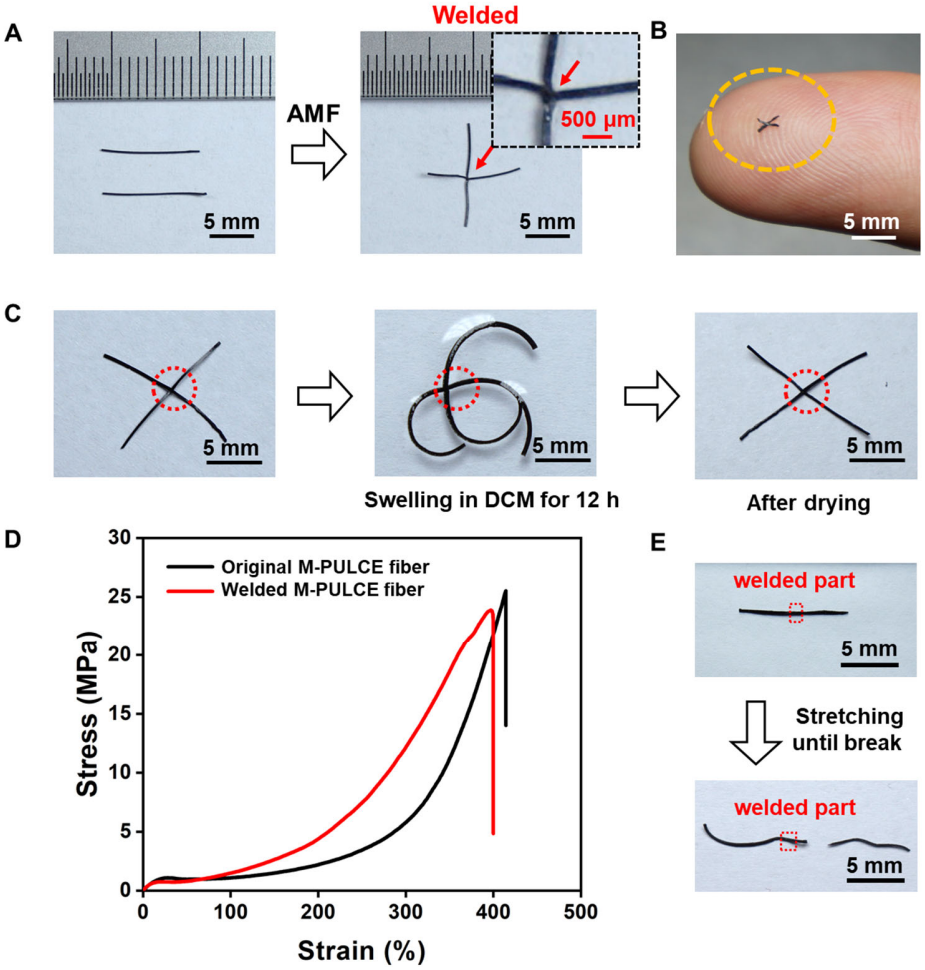

Fig. S12.

AMF-assisted welding of micro-scale M-PULCE-2 fibers. The cross-section dimension of all the fibers shown here is 160 μm × 120 μm (width × thickness). (**A**) Images of M-PULCE fibers before and after welding. The red arrow indicates the welding region. The overlapped area is 160 μm × 160 μm. (**B**) Image of a welded M-PULCE fiber on a fingertip. The original length of the fiber before welding is 2.65 mm. (**C**) Swelling experiment of the welded structure in solvent DCM. The welded joint remained intact during and after swelling. The welded area is circled by the dotted box. (**D**) Lap-shear test of the original M-PULCE fiber and the AMF-welded fiber (sample size: 160 μm × 120 μm (width × thickness); overlapped area: 160 μm × 160 μm). (**E**) The welded fiber before and after the tensile test. The break is outside the welded region.

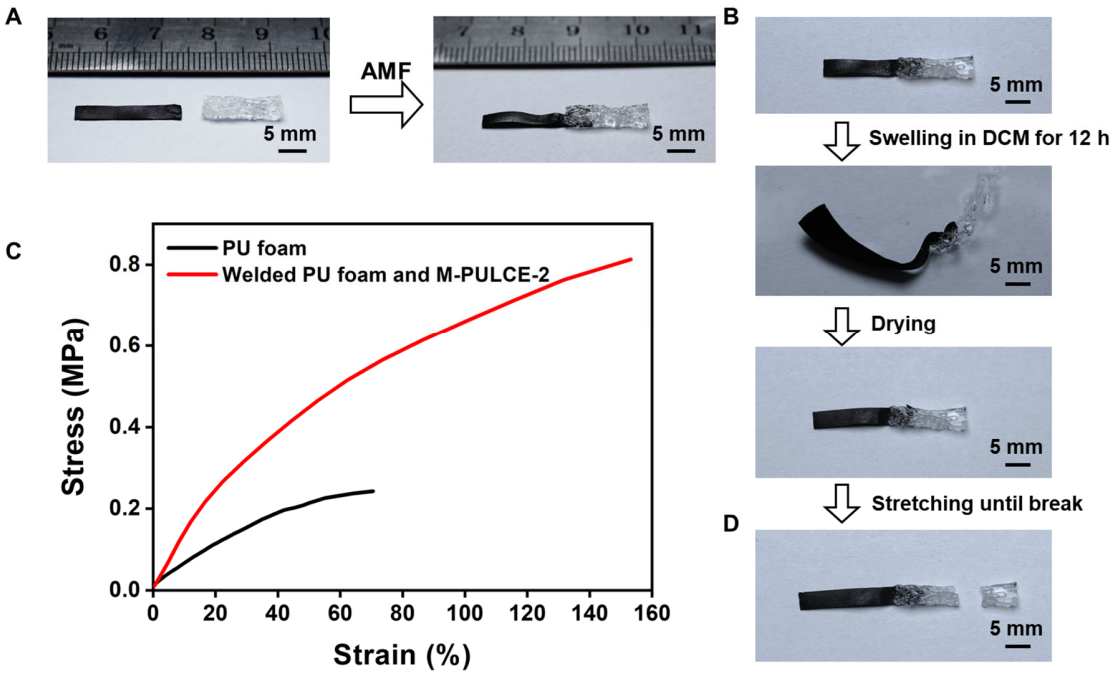

Fig. S13.

AMF-assisted welding of PU foam and M-PULCE-2. (**A**) Images of the bulk PU foam (dimension: 18.98 mm × 3.23 mm × 0.27 mm) and the M-PULCE film (dimension: 14.06 mm × 3.27 mm × 2.69 mm) before and after welding. (**B**) Swelling experiments of the welded structure in solvent DCM. (**C**) Lap-shear test of the original PU foam and the welded composite. (**D**) The welded composite after being stretched until fracture. The break occurred on the bulk foam.

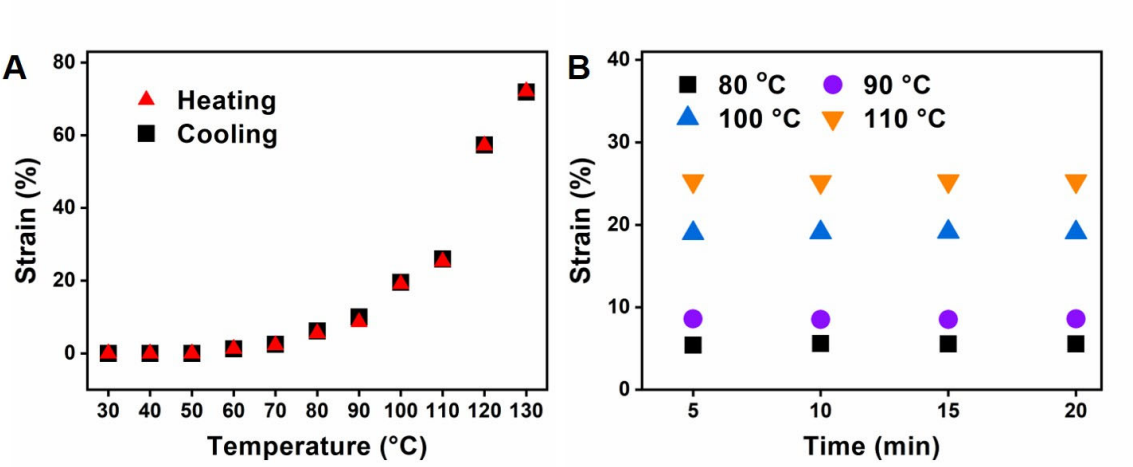

Fig. S14.
Stepwise control of M-PULCEs. (**A**) Corresponding actuation strains of the monodomain M-PULCE-2 sample at different temperatures (from 30 ºC to 130 ºC) on a precise hot plate in the heating and cooling cycle. Under 70 ºC, the shape change is almost negligible, less than 2%. Most of the length change (5%-72%) occurred between 80 ºC and 130 ºC, so there are 6 distinct intermediate states accessible in the whole actuation process. (**B**) Actuation strains of the sample at given temperatures (80, 90, 100, and 110 ºC) during 20 minutes.

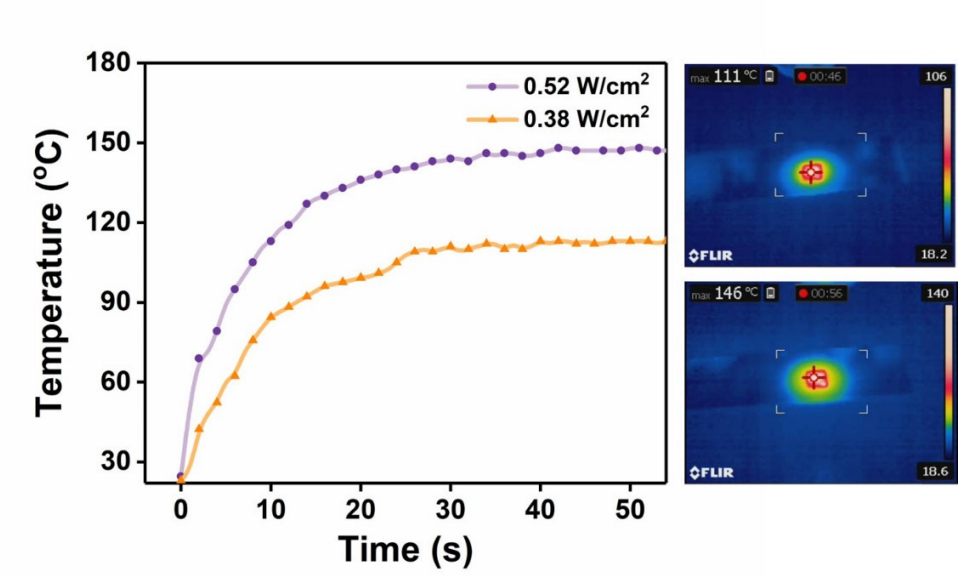

Fig. S15.

Temperature increase curves of M-PULCE-2 under different intensities of NIR irradiation (0.38 W/cm^2 and 0.52 W/cm^2). Right: IR thermal images of a M-PULCE-2 sample under 0.38 W/cm^2 (above) and 0.52 W/cm^2 (below) NIR irradiation. The temperatures on the focal point are 111 ºC and 146 ºC respectively.

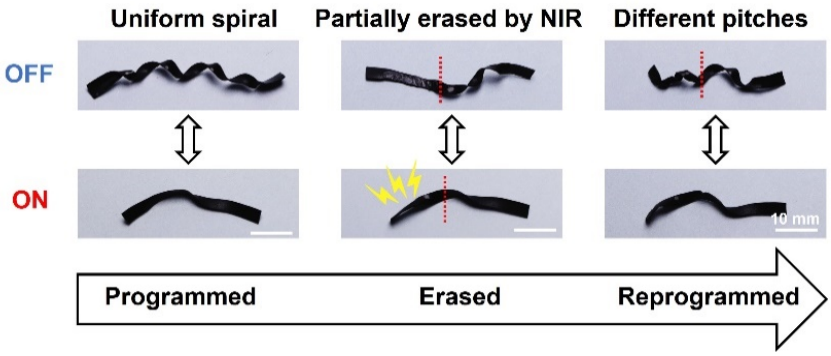

Fig. S16.

Partially reprogramming and erasing the programmed motion of M-PULCEs by NIR. M-PULCE-2 was programmed with a uniformly spiraling/straightening motion at first. For partially erasing, the left half of the actuator was irradiated by NIR (0.52 W/cm^2) for 20 minutes and the right half was covered with an opaque mask. The installed mesogen order on the left half was removed by this process but that on the right half remained. Then, the left half was reprogrammed into a spiral with a smaller pitch by the same NIR.

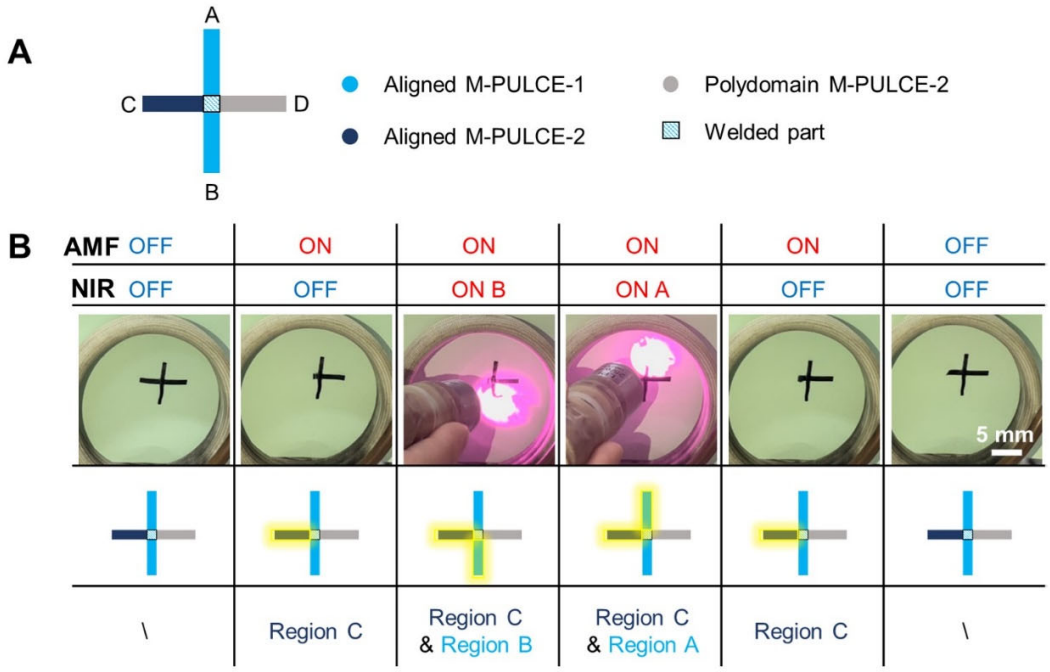

Fig. S17.

Welded M-PULCE actuator controlled by NIR and AMF simultaneously. (**A**) Composition of the welded actuator. (**B**) Welded M-PULCE actuator controlled by NIR and AMF simultaneously. When AMF (f = 320 kHz, H = 219.27 Gs) was ON, only the temperature of M-PULCE-2 (with higher Fe_3O_4 content; the magneto-thermal effect is stronger than M-PULCE-1) reached T_i, inducing bending of region C. Then the NIR light (intensity: 0.40 W/cm^2) was shined on region B and A respectively, they responded in turn; as the AMF was still ON, region C was still bending. After switching off the AMF and NIR, the whole sample went back to the original 2D geometry.

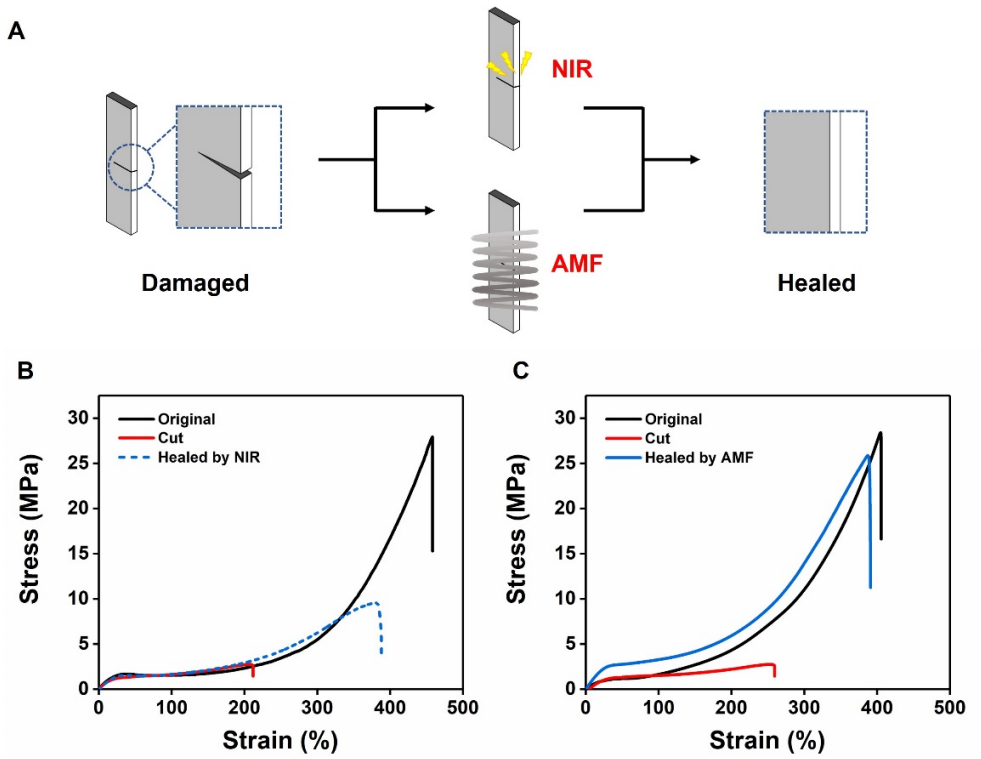

Fig. S18.

Self-healing by NIR and AMF. (**A**) Schematic illustration of NIR and AMF-assisted healing process. (**B**) Stress-strain curves of the original, half-cut, and NIR-healed M-PULCE-2 samples. (**C**) Stress-strain curves of the original, half-cut, and AMF-healed M-PULCE-2 samples.

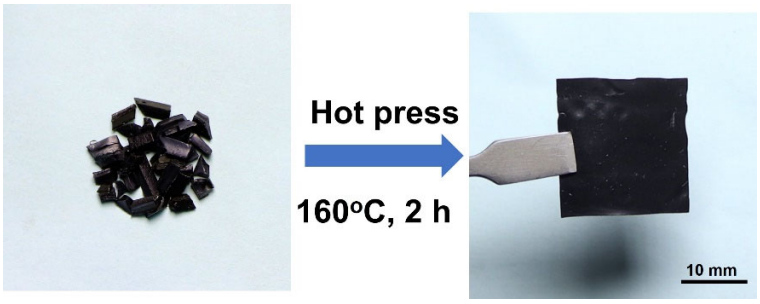

Fig. S19.

Remolding multiple pieces of three programmed actuators into a polydomain M-PULCE sample. Three programmed actuators composed of M-PULCE-2 were chopped into many pieces (left), then placed in a square mold and hot-pressed at 160 ºC for 2 h under a pressure of 10 MPa. After cooling down, a recycled film of polydomain M-PULCE-2 was obtained (size: 21.3 mm × 22.1 mm ×0.8 mm).

Sample	PULCE	M-PULCE-1	M-PULCE-2	M-PULCE-3
Gel content (wt%)	97.17	97.56	95.22	96.57

Table S1.

Gel content for PULCE and M-PULCE samples.

Sample	PULCE	M-PULCE-1	M-PULCE-2	M-PULCE-3
Stretching ration	180%	180%	180%	180%
Max actuation strain	90%	72%	78%	60%

Table S2.

Maximum actuation strains of PULCE and M-PULCE samples with different contents of Fe_3O_4 NPs.

Movie S1.

Dynamic satellite-memetic multimaterial structure under AMF.

Movie S2.

Octopus-like multimaterial soft robot with eight legs showing reversible curling/straightening motions under AMF.

Movie S3.

The magneto-responsive actuator without the welded foam “head” sinking in the water.

Movie S4.

The octopus-like M-PULCE actuator with the foam “head” welded seamlessly floating on the water.

Movie S5.

The demonstration of local control by magnetics in the assembled hand-like actuator.